Analysis of the timescale separation is required in order to improve the SPT formulation of the problem and consequently the results.

References

[1]Katz, A., *Subsonic Airplane Performance*, Society of Automotive Engineers, Warrendale, PA, 1994, pp. 3–9.

[2]Visser, H. G., "An Introduction to the Technique of Singular Perturbation Applied to Performance Optimization Problems in Atmospheric Flight Mechanics," Delft Univ. of Technology, Dept. of Aerospace Engineering, Rept. LR-374, The Netherlands, Dec. 1982.

[3]Naidu, D. S., and Calise, A. J., "Singular Perturbation and Time Scales in Guidance and Control of Aerospace Systems: A Survey," *Journal of Guidance, Control, and Dynamics*, Vol. 24, No. 6, 2001, pp. 1057–1078.

[4]Visser, H. G., and Shinar, J., "A Highly Accurate Feedback Approximation for Horizontal Variable-Speed Interceptions," *Journal of Guidance, Control, and Dynamics*, Vol. 9, No. 6, 1986, pp. 691–698.

[5]Ardema, M. D., and Rajan, N., "Separation of Time Scales in Aircraft Trajectory Optimization," *Journal of Guidance, Control, and Dynamics*, Vol. 8, No. 2, 1985, pp. 275–278.

[6]Kelley, H. J., "Aircraft Maneuver Optimization by Reduced Order Approximation," *Control and Dynamic Systems*, edited by C. T. Leondis, Vol. 10, Academic Press, New York, 1973, pp. 131–178.

[7]Sheu, D., Chen, Y.-M., and Chern, Jeng-Shing, "Optimal Glide for Maximum Reachable Domain," AIAA Paper 98-4462, Aug. 1999.

Modern Explicit Guidance Law for High-Order Dynamics

S. H. Jalali-Naini*
Aerospace Research Institute, 14657 Tehran, Iran

I. Introduction

OPTIMAL control theory has been utilized to derive modern guidance laws with improved performance. This is an attempt to replace the well-known proportional navigation (PN). The requirement for better performance has led to the development of optimal guidance laws (OGLs) by the consideration of the target future maneuver and the dynamics of an interceptor and its target from perfect to time-invariant high-order autopilots.[1–4]

The desired performance index in the exoatmosphere is usually the amount of fuel required for corrective maneuvers. If the fuel consumption were minimized, the solution would be mathematically intractable,[1] especially with trajectory constraints. Explicit guidance laws (EGLs) may be developed to deal with this objective function. The original idea of the EGLs comes from Cherry, who developed a zero-miss guidance from a given time history of acceleration command assuming a vehicle with perfect dynamics.[5] Later, a zero-miss EGL was presented to improve autopilot lag compensation for arbitrary-order autopilots. Blackburn obtained a closed-loop terminal guidance for a PN-like acceleration profile for time-invariant autopilots.[6] This type of acceleration profile is not suitable for nonminimum phase autopilots.

Depending on specified mission, a midcourse strategy may be programmed.[7,8] Massoumnia developed an optimal midcourse strategy followed by a coasting phase for a perfect autopilot.[7] In this work, a nonzero-miss EGL is developed for an interceptor having a linear time-variant arbitrary-order autopilot. This approach is also extended for midcourse guidance strategies for two classes of systems. In addition, two classes of optimal midcourse guidance laws are obtained.[9,10] The proposed scheme, as well as the optimal control theory, assumes that the target future maneuvers are completely defined.

Received 18 October 2003; revision received 6 April 2004; accepted for publication 9 April 2004.

*Research Engineer, P.O. Box 14665-834. Senior Member AIAA.

II. Explicit Guidance Problem and Solution

A linear time-varying system is represented in the following state-space form:

$$\dot{\boldsymbol{X}} = A(t)\boldsymbol{X} + B(t)\boldsymbol{U} + \boldsymbol{C}(t) \tag{1}$$

where $\boldsymbol{X}(\cdot)$ is the state vector, $\boldsymbol{U}(\cdot)$ the control vector, $A(t)$ the system matrix, $B(t)$ the input matrix, and $\boldsymbol{C}(t)$ a time-varying vector. All vectors and matrices are of appropriate dimensions. The final state at the final time t_f is given by

$$\boldsymbol{X}(t_f) = \boldsymbol{\Phi}(t_f, t)\boldsymbol{X}(t) + \int_t^{t_f} \boldsymbol{\Phi}(t_f, \lambda)B(\lambda)\boldsymbol{U}(\lambda)\,\mathrm{d}\lambda + \int_t^{t_f} \boldsymbol{\Phi}(t_f, \lambda)\boldsymbol{C}(\lambda)\,\mathrm{d}\lambda \tag{2}$$

with $\boldsymbol{\Phi}(t, t_0)$ being the fundamental matrix. We are to reach the desired state $\boldsymbol{X}^*(t_f)$ at the final time. The final deviation from the desired final state is denoted by $\boldsymbol{M} = \boldsymbol{X}^*(t_f) - \boldsymbol{X}(t_f)$. The predicted error at the final time without effort, that is, $\boldsymbol{U}(\xi) = \boldsymbol{0}$, $t < \xi \leq t_f$, is expressed as

$$\boldsymbol{Z}(t) = \boldsymbol{X}^*(t_f) - \boldsymbol{\Phi}(t_f, t)\boldsymbol{X}(t) - \int_t^{t_f} \boldsymbol{\Phi}(t_f, \lambda)\boldsymbol{C}(\lambda)\,\mathrm{d}\lambda \tag{3}$$

Thus, we can write

$$\boldsymbol{M} = \boldsymbol{Z}(t) - \int_t^{t_f} \boldsymbol{\Phi}(t_f, \lambda)B(\lambda)\boldsymbol{U}(\lambda)\,\mathrm{d}\lambda \tag{4}$$

$$\boldsymbol{Z}(t) - \boldsymbol{Z}(t_0) = -\int_{t_0}^{t} \boldsymbol{\Phi}(t_f, \lambda)B(\lambda)\boldsymbol{U}(\lambda)\,\mathrm{d}\lambda \tag{5}$$

where the subscript 0 denotes the initial value. We are to construct a closed-loop guidance law from a given control history $\boldsymbol{U} = H(t)\boldsymbol{Z}(t_0)$, that is, H is given and its elements are piecewise continuous functions of time. Therefore, we have

$$\boldsymbol{Z}(t) = \left[I - \int_{t_0}^{t} \boldsymbol{\Phi}(t_f, \lambda)B(\lambda)H(\lambda)\,\mathrm{d}\lambda\right]\boldsymbol{Z}(t_0) \tag{6}$$

where I is the identity matrix. We assume that the expression in the brackets is invertible for $t_0 \leq t \leq t_f$. When the preceding relation is used, the closed-loop guidance law is obtained as

$$\boldsymbol{U} = H\left[\boldsymbol{W} + \int_t^{t_f} \boldsymbol{\Phi}(t_f, \lambda)B(\lambda)H(\lambda)\,\mathrm{d}\lambda\right]^{-1}\boldsymbol{Z}(t) \tag{7}$$

in which

$$\boldsymbol{W} = I - \int_{t_0}^{t_f} \boldsymbol{\Phi}(t_f, t)B(t)H(t)\,\mathrm{d}t \tag{8}$$

must satisfy the matrix equation $\boldsymbol{M} - \boldsymbol{W}\boldsymbol{Z}(t_0) = \boldsymbol{0}$ to reach the allowable predetermined final error $\boldsymbol{M}$. When the mentioned formulation is used, the EGL for final position and/or velocity constraints can be obtained for time-variant arbitrary-order autopilots. For this purpose, the elements of the guidance gain matrix corresponding to the states with unconstrained final values are set to zero.[9]

III. Derivation of Modern Guidance Laws

Assume that we have the following relation between the predetermined miss distance $\boldsymbol{m}_p$, zero-effort miss (**ZEM**) and commanded acceleration $\boldsymbol{u}$ ($m_p < \mathrm{ZEM}_0$):

$$\boldsymbol{m}_p - \mathbf{ZEM}(t) = -\int_t^{t_c} \alpha(\xi)\boldsymbol{u}(\xi)\,\mathrm{d}\xi \qquad t_0 \le t \le t_c \tag{9}$$

where t_c is a specified time, $\alpha(t)$ is continuous, $m_p = |\boldsymbol{m}_p|$, and $\mathrm{ZEM} = |\mathbf{ZEM}|$. The commanded acceleration is assumed to be zero for $t > t_c$. Now, the problem is twofold.

1) What is the OGL to minimize

$$\mathcal{J} = \int_t^{t_f} |\boldsymbol{u}|^2\,\mathrm{d}t$$

2) What is the closed-loop commanded acceleration for a given acceleration history?

Optimal Intercept Strategy

We are to obtain the nonzero-miss OGL subject to minimizing $\mathcal{J}$ under differential equation constraint $\dot{\mathbf{ZEM}}(t) = -\alpha(t)\boldsymbol{u}$ and final condition $\mathbf{ZEM}(t_c) = \boldsymbol{m}_p$. The **ZEM** will remain constant after $t = t_c$, so that we can consider t_c as the final time. Differentiating the Hamiltonian, $\mathcal{H} = \boldsymbol{u}^T\boldsymbol{u} - \boldsymbol{\lambda}^T\alpha(t)\boldsymbol{u}$, with respect to control input yields $\boldsymbol{u} = \frac{1}{2}\boldsymbol{\lambda}\alpha(t)$, where $\boldsymbol{\lambda}$ is the costate vector; $\boldsymbol{\lambda}$ is constant. The optimal command can then be found as

$$\boldsymbol{u} = \left[\alpha(t) \Big/ \int_t^{t_c} \alpha^2(\xi)\,\mathrm{d}\xi\right](\mathbf{ZEM} - \boldsymbol{m}_p) \tag{10}$$

Assuming $\boldsymbol{m}_p = k\mathbf{ZEM}_0$, $0 \le k < 1$ is constant, yields

$$\boldsymbol{u} = \left\{\alpha(t) \Big/ \left[\left(\frac{k}{1-k}\right)\int_{t_0}^{t_c} \alpha^2(t)\,\mathrm{d}t + \int_t^{t_c} \alpha^2(\xi)\,\mathrm{d}\xi\right]\right\}\ \mathbf{ZEM} \tag{11}$$

Explicit Intercept Strategy

We consider the commanded acceleration history in the form of $\boldsymbol{u} = f(t)\ \mathbf{ZEM}(t_0)$, where $f^*(t) = f(t)/f(t_0)$ is chosen by a guidance designer as a piecewise continuous function. Therefore, $\boldsymbol{m}_p$ must be proportional to $\mathbf{ZEM}_0$. Using Eq. (9), we arrive at

$$\boldsymbol{m}_p = \left[1 - \int_{t_0}^{t_c} \alpha(t) f(t)\,\mathrm{d}t\right]\mathbf{ZEM}(t_0) \tag{12}$$

$$\mathbf{ZEM}(t) = \left[1 - \int_{t_0}^{t} \alpha(\xi) f(\xi)\,\mathrm{d}\xi\right]\mathbf{ZEM}(t_0) \tag{13}$$

It is assumed that $f(t_0) \ne 0$ and $\alpha(t)f(t) \ge 0$. The commanded acceleration can then be obtained for $t_0 \le t \le t_c$ as

$$\boldsymbol{u} = f(t)\mathbf{ZEM} \Big/ \left[\left(\frac{m_p}{\mathrm{ZEM}_0 - m_p}\right)\int_{t_0}^{t_c} \alpha(t) f(t)\,\mathrm{d}t + \int_t^{t_c} \alpha(\xi) f(\xi)\,\mathrm{d}\xi\right] \tag{14}$$

Therefore, when $f(t)$ is proportional to $\alpha(t)$, $\mathcal{J}$ is minimized. The solution of $\boldsymbol{u}$ is given by

$$\boldsymbol{u} = \left[(\mathrm{ZEM}_0 - m_p) f^*(t) \Big/ \int_{t_0}^{t_c} \alpha(t) f^*(t)\,\mathrm{d}t\right]\boldsymbol{i}_{\mathrm{ZEM}_0} \tag{15}$$

where $\boldsymbol{i}_{\mathrm{ZEM}} = \mathbf{ZEM}/\mathrm{ZEM}$ is the unit vector along ZEM. The lateral divert,

$$\Delta V = \int_0^{t_f} |\boldsymbol{u}|\,\mathrm{d}t$$

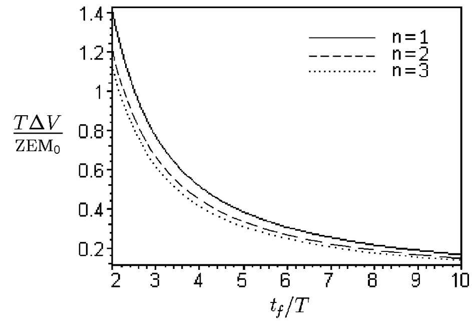

Fig. 1 Normalized lateral divert requirements vs final time.

can then be obtained for $m_p = 0$ and $t_0 = 0$ as

$$\Delta V = \left[\int_0^{t_c} |f(t)|\,\mathrm{d}t \Big/ \int_0^{t_c} \alpha(t) f(t)\,\mathrm{d}t\right]\mathrm{ZEM}_0 \tag{16}$$

For terminal guidance, we simply set $t_c = t_f$ in Eqs. (9–16).

IV. Terminal Guidance Laws

Differentiation of Eq. (9) implies that $f(t)$ and $\alpha(t)$ must be nonzero and of the same sign so that the commanded acceleration can reduce the ZEM at any time. The commanded acceleration is also most effective when it has larger values for larger values of $|\alpha(t)|$. The PN-like acceleration profile, $f^*(t) = (1 - t/t_f)^n$, is a good choice when $\alpha(t) \ge 0$ is a strictly monotonically decreasing function of time, $n \ge 0$ is a constant. When $\alpha(t)f(t) < 0$, a singularity problem may appear in the closed-loop commanded acceleration. The acceleration profile may be chosen proportional to $\mathrm{sgn}[\alpha(t)]|\alpha(t)|^n$ for minimum and nonminimum phase autopilots where $\mathrm{sgn}(\cdot)$ is the signum function.[11] The predetermined miss distance is also chosen nonzero to avoid the guidance gain approaching infinity at the end of steering period.

The solutions of ΔV for three values of n, where $n = 1, 2, 3$, and $m_p = 0$ are shown in normalized form in Fig. 1 for a linear first-order autopilot with time constant of T (Ref. 9). In this case, $f(t)$ is proportional to $(e^{-\tau} + \tau - 1)^n$ where $\tau = (t_f - t)/T$. Note that, for $n = 1$, $\mathcal{J}$ is minimized. Increasing n from one decreases the lateral divert requirements while it increases the initial acceleration command. In practice, the maximum value of n is limited by stability criteria. If the value of the acceleration command exceeds the acceleration limit, it will stay at the limit and may come off the limit later.

V. Midcourse Guidance Laws

We are now to develop midcourse strategies followed by a coasting phase without corrective maneuvers for perfect dynamics and two classes of systems.

Perfect Dynamics

For a zero-lag optimal strategy as treated by Massoumnia,[7] Eq. (11) simplifies to

$$\boldsymbol{u} = t_g\ \mathbf{ZEM} \Big/ \left\{\tfrac{1}{3}[m_p/(\mathrm{ZEM}_0 - m_p)]\left[t_f^3 - (t_f - t_c)^3\right] + t_{cg}\left(t_g^2 - t_g t_{cg} + \tfrac{1}{3}t_{cg}^2\right)\right\} \tag{17}$$

where $t_g = t_f - t$ and $t_{cg} = t_c - t$. To develop an EGL, one may choose $f^*(t) = (1 - t/t_c)^n$ for $t \le t_c$ (Ref. 8). As a special case of Eq. (14) for $\alpha(t) = t_g$, we obtain

$$\boldsymbol{u} = t_{cg}^n\ \mathbf{ZEM} \Big/ \left\{[m_p/(\mathrm{ZEM}_0 - m_p)][(t_g - t_{cg})/(n+1) + t_c \big/ (n+2)]t_c^{n+1} + [(t_g - t_{cg})/(n+1) + t_{cg}/(n+2)]t_{cg}^{n+1}\right\} \tag{18}$$

The lateral divert requirement for the explicit strategy for $m_p = 0$ is given by

$$\Delta V = \mathrm{ZEM}_0/[t_f - t_c/(n+2)] \tag{19}$$

The preceding relation implies that increasing n or decreasing t_c decreases the lateral divert requirements. Also, increasing n increases the initial commanded acceleration. Therefore, there is a tradeoff between saving ΔV and larger initial commanded acceleration.

First Class of Systems

Assume that the steering command is truncated at a specified time t_c, but the achieved commanded acceleration continues depending on the system's characteristics. In this case, Eq. (9) holds according to the Appendix. For a first-order, time-invariant autopilot, OGL simplifies to

$$\boldsymbol{u} = \frac{(1/T^2)(e^{-\tau} + \tau - 1)\,\mathbf{ZEM}}{[m_p/(\mathrm{ZEM}_0 - m_p)]Q_{so}(h_0, \tau_0) + Q_{so}(h, \tau)} \tag{20}$$

where $h = t_{cg}/T$, $h_0 = t_c/T$, $\tau_0 = t_f/T$, and

$$Q_{so}(h, \tau) = h\left(\tfrac{1}{3}h^2 - \tau h + h + \tau^2 - 2\tau + 1\right) + 2e^{-\tau}(\tau e^h - he^h - \tau) + \tfrac{1}{2}e^{-2\tau}(e^{2h} - 1) \tag{21}$$

The first-order EGL for $f^*(t) = (1 - t/t_c)$ until t_c simplifies to

$$\boldsymbol{u} = \frac{(h/T^2)\mathbf{ZEM}}{[m_p/(\mathrm{ZEM}_0 - m_p)]Q_{se}(h_0, \tau_0) + Q_{se}(h, \tau)} \tag{22}$$

where

$$Q_{se}(h, \tau) = -\tfrac{1}{6}h^3 + \tfrac{1}{2}h^2(\tau - 1) + e^{-\tau}(e^h - h - 1) \tag{23}$$

Second Class of Systems

In the second class, the corrective maneuvers are cut off at $t = t_b$, regardless of the commanded acceleration, that is, the achieved commanded acceleration is zero for $t > t_b$. The commanded acceleration does not affect the trajectory after t_b; therefore, to apply the results of Sec. III, we may assume $\boldsymbol{u} = \mathbf{0}$ for $t > t_b$.

The OGL for a linear time-invariant, first-order autopilot is obtained as

$$\boldsymbol{u} = \frac{(1/T^3)\alpha(t)\mathbf{ZEM}}{[m_p/(\mathrm{ZEM}_0 - m_p)]Q'_{so}(h'_0, \tau_0) + Q'_{so}(h', \tau)} \tag{24}$$

where

$$Q'_{so}(h', \tau) = \tfrac{1}{3}h'^3 - c_b h'^2 + c_b^2 h' - \tfrac{1}{2}c_b^2 e^{-2h'} - 2c_b(h' + 1 - c_b)e^{-h'} - \tfrac{3}{2}c_b^2 + 2c_b \tag{25}$$

and $h' = t_{bg}/T$, $h'_0 = t_b/T$, $c_b = 1 + h' - \tau$, and $\alpha(t) = T(c_b e^{-h'} + \tau - 1)$; see the Appendix.

To develop the first-order EGL, we choose $f^*(t) = (1 - t/t_b)^n$ for $t \le t_b$ to yield, for $n = 1$,

$$\boldsymbol{u} = \frac{(h'/T^2)\,\mathbf{ZEM}}{[m_p/(\mathrm{ZEM}_0 - m_p)]Q'_{se}(h'_0, \tau_0) + Q'_{se}(h', \tau)} \tag{26}$$

where

$$Q'_{se}(h', \tau) = \tfrac{1}{3}h'^3 - \tfrac{1}{2}c_b h'^2 - c_b(1 + h')e^{-h'} + c_b \tag{27}$$

VI. Simulation Results

For a computer simulation, we use the equations and assumptions given in the Appendix. The dynamic of the interceptor is modeled as a single lag with a time constant of 0.3 s. The constant model for gravitational acceleration, $\boldsymbol{g} = [0,0,\text{-}9.81]^T$ m/s^2, is assumed and $\boldsymbol{c}(t) = \boldsymbol{g}$. Suppose an interceptor at the origin having an initial vertical velocity of 1500 m/s is to reach the target position of $\boldsymbol{r}^*(t_f) = [35, 35, 20]^T$ km at $t_f = 30$ s and its steering period is 10 s.

The absolute values of the commanded accelerations of three guidance laws with $t_c = 10$ s and their corresponding achieved accelerations are shown in Fig. 2 for system 1. Zero-lag OGL with

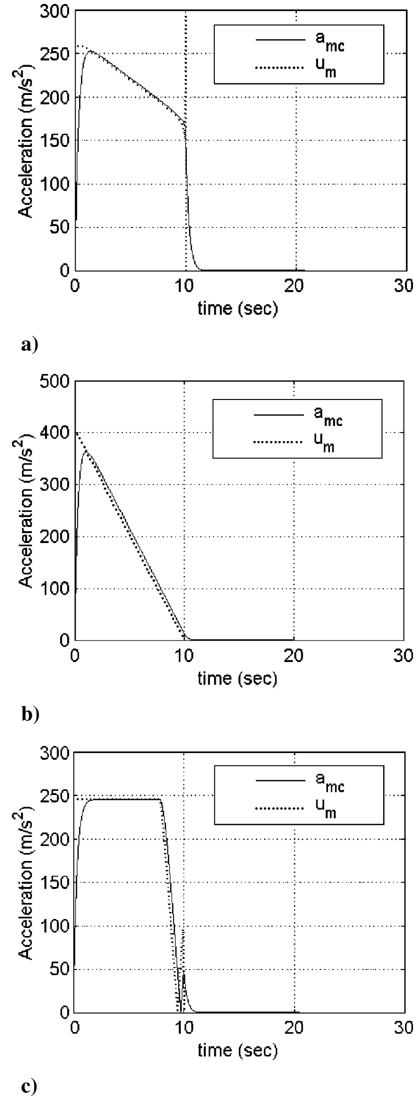

Fig. 2 Acceleration history for system 1: a) zero-lag OGL, b) first-order EGL, and c) zero-lag EGL.

$m_p = 0.1$ m produces a miss distance of 502 m with required lateral divert of 2177 m/s. The first-order OGL has been developed to compensate the miss distance of the zero-lag OGL. It requires a lateral divert of 2141 m/s to produce zero-miss distance. The acceleration profiles of the two OGLs are almost similar, except the zero-lag OGL has a peak at $t = 10$ s as shown in Fig. 2a. The EGLs are developed to reduce the lateral divert requirement and to shape the acceleration command. The first-order EGL commanded acceleration at $t_c = 10$ turns out to be zero, which is a better behavior than the optimal one (Fig. 2b). The first-order EGL needs a lateral divert of 2035 m/s to produce zero-miss distance. Therefore, the EGL requires less fuel consumption than that of the optimal strategy, but it needs more g-level capability. For the same g-level capability as the OGL, the required lateral divert is 2098 m/s, which is still smaller than that of the optimal one. Increasing n and the acceleration limit, and also increasing t_c until a limit, increases the difference between the fuel consumptions of the two guidance laws for a specified final time. For example, the lateral divert requirements of first-order explicit and optimal strategies for $t_c = 15$ s and the same g-level capability of 21 are 2229 and 2326 m/s, respectively. Note that the OGL minimizes $\mathcal{J}$, not the integral of $|\boldsymbol{u}|$.

Now, consider the zero-lag EGL with Eq. (18) for $m_p = 0.1$ m and $n = 1$. This guidance law produces miss distance of 69 m without acceleration limit and requires a lateral divert of 2030 m/s. With an acceleration limit of 25 g as shown in Fig. 2c, miss distance increases to 270 m, whereas the first-order EGL produces zero-miss distance. For zero-lag EGL, miss distance normally increases as the slope of

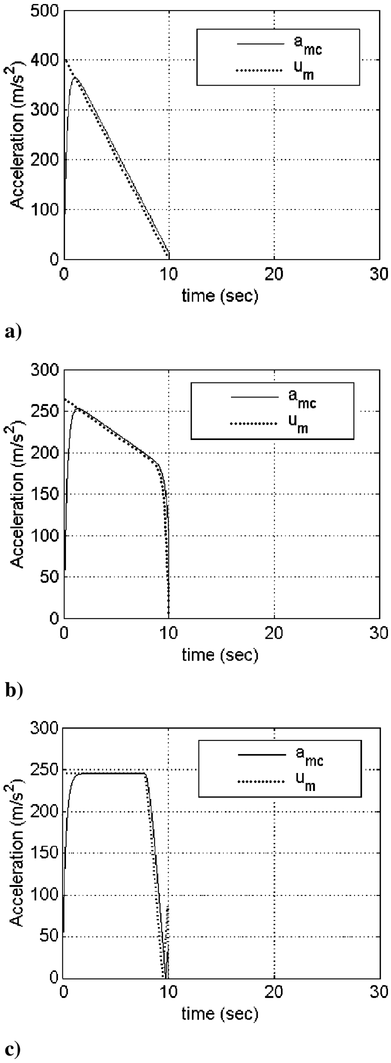

Fig. 3 Acceleration history for system 2: a) first-order EGL, b) first-order OGL, and c) zero-lag EGL.

the acceleration profile steepens. The lateral divert requirements of zero-lag and first-order explicit (optimal) guidance laws are very similar. The first-order strategies produce less miss distance that those of the zero-lag guidance laws.

The acceleration profiles of three guidance laws are shown in Fig. 3 for system 2 with $t_b = 10$ s. The required lateral divert for the first-order EGL and OGL are 2037 and 2152 m/s, respectively. The EGL reduces the fuel consumption, depending on the g-level capability of an interceptor. As shown in Fig. 3a, the EGL commanded acceleration zeros out at the end of the steering period, whereas the optimal steering may have a considerable value at this time (Fig. 3b). This leads to a better behavior for the EGL. The acceleration profile of the zero-lag OGL for $m_p = 0.1$ m and its miss distance are very similar to those of first-order OGL, but they are very sensitive to the estimation error of t_b. For example, if the estimation of t_b is 10.05 s and $m_p = 0.1$ m, miss distance will increase to 147 and 94 m for zero-lag and first-order OGLs and 7 and 13 m for zero-lag and first-order EGLs, respectively. When an acceleration limit of 25 g is applied in this case, the miss distance will increase to 26 and 28 m for zero-lag and first-order EGLs, respectively. As shown in Fig. 3c, the zero-lag EGL acceleration reverses its direction. The lateral divert requirements and miss distance of zero-lag and first-order EGLs are very similar for system 2. The performances of zero-lag strategies for system 2 are better than those of system 1. This is because the ZEM relation of system 2 for first-order strategies tends to that of zero-lag strategies as $t_b - t$ goes to zero. The zero-lag EGL works well for the second class, but the commanded acceleration reverses its direction in the last instants of the steering period, which is impractical in many systems. When the explicit method is used, the acceleration profile can be shaped in the last moments according to specific propulsion dynamics. EGLs produce less miss distance than those of the optimal ones. As a rule of thumb miss distance is equal to $(t_f - t_b)$ per unit velocity error at $t = t_b$. This means that the resulted miss distance increases for larger coasting phase duration. When EGLs are used, the amount of fuel provided for the terminal phase can also be reduced.

VII. Conclusions

The main contribution of this work is to introduce a systematic method for developing explicit/optimal midcourse/terminal guidance laws for time-variant, arbitrary-order autopilots against maneuvering targets. This method enables guidance designers to develop a nonzero-miss explicit guidance for a given time history of commanded acceleration for minimum and nonminimum phase autopilots. To develop midcourse guidance laws, two classes of systems are considered here. First, the acceleration command is truncated at a specified time. Second, the corrective maneuvers are cut off at a specified time, regardless of the acceleration commands, for example, at burnout. The optimal strategies with the least integral of the squared control effort are then obtained for the two classes. The ZEM relations for explicit and optimal guidance laws are the same, but the guidance gains are different. The ZEM is not dependent on the steering period for the first class, whereas it depends on burnout time for the second class. The OGLs are compared with their corresponding explicit strategies for perfect and first-order autopilots. The explicit strategies have better acceleration profiles and less fuel consumptions than those of the OGLs with the least integral of square of the acceleration command.

Appendix: ZEM

Consider an interceptor having velocity $\boldsymbol{v}$ pursuing its target with respect to an inertial reference $(Oxyz)$. The governing equation of motion for the interceptor is $\ddot{\boldsymbol{r}} = \boldsymbol{c}(t) + \boldsymbol{a}_c$, where $\boldsymbol{r}$ and $\boldsymbol{a}_c$ are the interceptor position and achieved commanded acceleration, respectively. Also, $\boldsymbol{c}(t)$ is the acceleration acting on the interceptor, excluding $\boldsymbol{a}_c$. We assume that $\boldsymbol{c}(t)$ is given as a vectorial function of time. We are to reach the desired final position $\boldsymbol{r}^*(t_f)$. If we are to intercept a maneuvering target, the desired interceptor final position must be the target final position.

First-Order Autopilot

The ZEM for a time-variant, first-order autopilot described by $\dot{\boldsymbol{a}}_c + \boldsymbol{a}_c/T(t) = \boldsymbol{u}/T(t)$ is obtained as

$$\mathbf{ZEM}(t) = \boldsymbol{r}^*(t_f) - \boldsymbol{r} - \boldsymbol{v}t_g - T(t)\alpha(t)\boldsymbol{a}_c - \int_t^{t_f} (t_f - \xi)\, \boldsymbol{c}(\xi)\, \mathrm{d}\xi \tag{A1}$$

where $T(t)$ is the time-dependent autopilot lag and

$$\alpha(t) = \frac{1}{T(t)} \int_t^{t_k} (t_f - \xi) \exp\left[- \int_t^{\xi} T^{-1}(\eta)\, \mathrm{d}\eta \right] \mathrm{d}\xi \tag{A2}$$

For the first class of systems, we have $t_k = t_f$, whereas $t_k = t_b$ for the second class.

High-Order Autopilot

We assume the interceptor autopilot is identical for each axis x, y, and z. This leads to three identical solutions for x, y, and z axes. The dynamics of the n'th-order autopilot in the y channel can be shown in a partitioned form as[4]

$$\begin{bmatrix} \dot{a}_{yc} \\ \dot{\boldsymbol{p}} \end{bmatrix} = \begin{bmatrix} a_{11}(t) & \boldsymbol{a}_{12}(t) \\ \boldsymbol{a}_{21}(t) & \boldsymbol{a}_{22}(t) \end{bmatrix} \begin{bmatrix} a_{yc} \\ \boldsymbol{p} \end{bmatrix} + \begin{bmatrix} b_1(t) \\ \boldsymbol{b}_2(t) \end{bmatrix} u_y \tag{A3}$$

where a_{yc} is the first state variable and $\boldsymbol{p}$ elements are the remaining $n' - 1$ state variables; a_{11} and b_1 are scalars; $\boldsymbol{a}_{21}$, $\boldsymbol{a}_{12}^T$, and $\boldsymbol{b}_2$ are

$(n'-1)\times 1$ vectors; $\boldsymbol{a}_{22}$ is a $(n'-1)\times(n'-1)$ matrix; and the subscript y represents the component along y axis. The fundamental matrix of the autopilot, if obtainable, is expressed as

$$\boldsymbol{\Phi}^A(t,t_0)=\begin{bmatrix}\boldsymbol{\Phi}_{11}^A(t,t_0) & \boldsymbol{\Phi}_{12}^A(t,t_0)\\ \boldsymbol{\Phi}_{21}^A(t,t_0) & \boldsymbol{\Phi}_{22}^A(t,t_0)\end{bmatrix} \tag{A4}$$

where $\boldsymbol{\Phi}_{11}^A$ is scalar, $\boldsymbol{\Phi}_{21}^A$ and $\boldsymbol{\Phi}_{12}^{A^T}$ are $(n'-1)\times 1$ vectors, and $\boldsymbol{\Phi}_{22}^A$ is a $(n'-1)\times(n'-1)$ matrix. The ZEM for the interceptor is obtained as

$$\begin{aligned}\mathrm{ZEM}_y &= y^*(t_f)-y-\nu t_g-\int_t^{t_f}(t_f-\xi)c_y(\xi)\,\mathrm{d}\xi\\ &-\left[\int_t^{t_k}(t_f-\xi)\boldsymbol{\Phi}_{11}^A(\xi,t)\,\mathrm{d}\xi \quad \int_t^{t_k}(t_f-\xi)\boldsymbol{\Phi}_{12}^A(\xi,t)\,\mathrm{d}\xi\right]\begin{bmatrix}a_{yc}\\ \boldsymbol{p}\end{bmatrix}\end{aligned} \tag{A5}$$

where $\nu=\dot{y}$. Differentiating the preceding relation yields the relation $\dot{\mathrm{ZEM}}_y=-\alpha(t)u_y$ where

$$\begin{aligned}\alpha(t) &= b_1(t)\int_t^{t_k}(t_f-\xi)\boldsymbol{\Phi}_{11}^A(\xi,t)\,\mathrm{d}\xi\\ &+\left[\int_t^{t_k}(t_f-\xi)\boldsymbol{\Phi}_{12}^A(\xi,t)\,\mathrm{d}\xi\right]\boldsymbol{b}_2(t)\end{aligned} \tag{A6}$$

Thus, we can write $\dot{\mathbf{ZEM}}(t)=-\alpha(t)\boldsymbol{u}$, which integrates for the first class into

$$\boldsymbol{m}=\mathbf{ZEM}(t)-\int_t^{t_c}\alpha(\xi)\boldsymbol{u}(\xi)\,\mathrm{d}\xi \tag{A7}$$

Therefore, Eq. (9) holds for the first class. The preceding relation is valid for the second class when we substitute t_b instead of t_c in this relation. Therefore, the results of Sec. III are applicable for the two classes of systems.

In the case that A and B are time invariant and $t_0=0$, Eq. (5A) simplifies to

$$\begin{aligned}\mathrm{ZEM}_y &= y^*(t_f)-y-\nu t_g-\int_t^{t_f}(t_f-\xi)c_y(\xi)\,\mathrm{d}\xi\\ &-\left\{\mathcal{L}^{-1}\left[\tilde{R}(s)\frac{\tilde{a}_{yc}(s)}{a_{yc}(0)}\right]\Bigg|_{t_k-t}\ \mathcal{L}^{-1}\left[\tilde{R}(s)\frac{\tilde{a}_{yc}(s)}{\boldsymbol{p}(0)}\right]\Bigg|_{t_k-t}\right\}\begin{bmatrix}a_{yc}\\ \boldsymbol{p}\end{bmatrix}\end{aligned} \tag{A8}$$

where s is the Laplace domain variable, $\mathcal{L}^{-1}$ is the inverse Laplace transform operator, $\tilde{a}_{yc}(s)/a_{yc}(0)=\tilde{\boldsymbol{\Phi}}_{11}^A(s)$ and $\tilde{a}_{yc}(s)/\boldsymbol{p}(0)=\tilde{\boldsymbol{\Phi}}_{12}^A(s)$, $\tilde{R}(s)=s^{-2}+(t_f-t_k)s^{-1}$, and the superscript tilde indicates the Laplace transform. We also have

$$\alpha(t)=\mathcal{L}^{-1}\left[\frac{1+(t_f-t_k)s}{s^2}\frac{\tilde{a}_{yc}(s)}{\tilde{u}_y(s)}\right]\Bigg|_{t_k-t} \tag{A9}$$

where $\tilde{a}_{yc}(s)/\tilde{u}_y(s)$ is the autopilot transfer function for the y channel. Note that the two classes of systems are identical for a perfect autopilot.

References

[1]Zarchan, P., *Tactical and Strategic Missile Guidance*, 3rd ed., Progress in Astronautics and Aeronautics, Vol. 176, AIAA, Reston, VA, 1997, Chap. 8.

[2]Hough, M. E., "Optimal Guidance and Nonlinear Estimation for Interception of Accelerating Targets," *Journal of Guidance, Control, and Dynamics*, Vol. 18, No. 5, 1995, pp. 959–968.

[3]Cottrell, R. G., "Optimal Intercept Guidance for Short-Range Tactical Missiles," *AIAA Journal*, Vol. 9, No. 7, 1971, pp. 1414, 1415.

[4]Rusnak, I., and Meir, L., "Optimal Guidance Law for Acceleration Constrained Missile and Maneuvering Target," *IEEE Transactions on Aerospace and Electronic Systems*, Vol. 26, No. 4, 1990, pp. 618–624.

[5]Cherry, G. W., "A General, Explicit, Optimizing Guidance Law for Rocket-Propelled Spaceflight," AIAA Paper 64-638, Aug. 1964.

[6]Blackburn, T. R., "Method for Improving Autopilot Lag Compensation in Intercept Guidance," *Journal of Guidance, Control, and Dynamics*, Vol. 19, No. 3, 1996, pp. 724–726.

[7]Massoumnia, M.-A., "Optimal Midcourse Guidance Law for Fixed-Interval Propulsive Maneuvers," *Journal of Guidance, Control, and Dynamics*, Vol. 18, No. 3, 1995, pp. 465–470.

[8]Jalali-Naini, S. H., and Ebrahimi, B., "Modified Guidance with N-Fixed-Interval Propulsive Maneuvers," AIAA Paper 2002-4951, Aug. 2002.

[9]Jalali-Naini, S. H., "Generalized Explicit Guidance Law for Time-Variant High-Order Dynamics," *Proceedings of the 4th Iranian Aerospace Society Conference*, Iranian Aerospace Society, Tehran, Iran, 2003, pp. 249–261.

[10]Jalali-Naini, S. H., "Modern Midcourse Guidance Law with High-Order Dynamics," AIAA Paper 2003-5356, Aug. 2003.

[11]Jalali-Naini, S. H., and Pourtakdoust, S. H., "Modern Guidance Laws Based on Minimum Fuel Consumption," *Proceedings of the 5th Iranian Aerospace Society Conference*, Iranian Aerospace Society, Tehran, Iran, 2004, pp. 221–232.

Methods for Compensating for Control Allocator and Actuator Interactions

Michael W. Oppenheimer* and David B. Doman†
U.S. Air Force Research Laboratory,
Wright–Patterson Air Force Base, Ohio 45433-7531

Introduction

NUMEROUS control allocation algorithms have been developed for aircraft for the purpose of providing commands to suites of control effectors to produce desired moments or accelerations. A number of approaches have been developed that ensure that the commands provided to the effectors are physically realizable. These actuator command signals are feasible in the sense that they do not exceed hardware rate and position limits. Buffington[1] developed a linear programming-based approach that separately considered cases where sufficient control power was available to meet a moment demand and a control deficiency case where the moment deficiency was minimized. Bodson[2] developed a linear programming approach where the sufficiency and deficiency branches were considered simultaneously, which resulted in computational savings. Quadratic programming approaches have also been considered.[3] In the early 1990s, Durham[4,5] developed a constrained control allocation approach called direct allocation that was based on geometric concepts of attainable moment sets. Page and Steinberg[6] as well as Bodson[2] have presented excellent survey papers that compare and contrast many of the control allocation approaches developed over the last two decades. Recent work in the area has resulted in the development of control allocation algorithms that can accommodate cases where the moments or accelerations produced by the control effectors are nonlinear functions of the effector position.[7,8]

A review of the constrained control allocation literature shows that the coupling effects that result from combining constrained

Received 11 December 2003; revision received 9 April 2004; accepted for publication 14 April 2004.

*Electronics Engineer, Control Theory and Optimization Branch, 2210 Eighth Street, Building 146, Room 305; Michael.Oppenheimer@wpafb.af.mil. Member AIAA.

†Senior Aerospace Engineer, Control Theory and Optimization Branch, 2210 Eighth Street, Building 146, Room 305; David.Doman@wpafb.af.mil. Senior Member AIAA.